

# Knockout of *Sirt2* alleviates traumatic brain injury in mice

Wei Wang, Qiu-Yuan Gong, Lin Cai, Yao Jing, Dian-Xu Yang, Fang Yuan, Hao Chen, Heng-Li Tian\*

<https://doi.org/10.4103/1673-5374.346457>

Date of submission: September 15, 2021

Date of decision: January 18, 2022

Date of acceptance: April 16, 2022

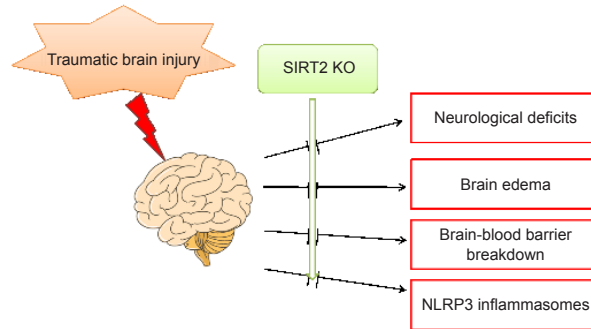
Date of web publication: June 2, 2022

## From the Contents

Introduction	350
Methods	350
Results	352
Discussion	353

## Graphical Abstract

Knockout of *SIRT2* alleviates neurological dysfunction induced by TBI via NLRP3/caspase-1 pathway



## Abstract

Sirtuin 2 (*SIRT2*) inhibition or *Sirt2* knockout in animal models protects against the development of neurodegenerative diseases and cerebral ischemia. However, the role of *SIRT2* in traumatic brain injury (TBI) remains unclear. In this study, we found that knockout of *Sirt2* in a mouse model of TBI reduced brain edema, attenuated disruption of the blood-brain barrier, decreased expression of the nucleotide-binding oligomerization domain-like receptor protein 3 (NLRP3) inflammasome, reduced the activity of the effector caspase-1, reduced neuroinflammation and neuronal pyroptosis, and improved neurological function. Knockout of *Sirt2* in a mechanical stretch injury cell model *in vitro* also decreased expression of the NLRP3 inflammasome and pyroptosis. Our findings suggest that knockout of *Sirt2* is neuroprotective against TBI; therefore, *Sirt2* could be a novel target for TBI treatment.

**Key Words:** blood-brain barrier; caspase-1; cerebral edema; neuroinflammation; neuroprotection; NLRP3; pyroptosis; *Sirt2*; tight junction protein; traumatic brain injury

## Introduction

Traumatic brain injury (TBI) is a complex disease process that includes primary injury and secondary injury (Morganti-Kossmann et al., 2019). Primary injury is caused by an initial direct mechanical force; secondary injury is caused by a series of pathophysiological changes induced by the primary injury, including neuroinflammation, blood-brain barrier (BBB) disruption, oxidative stress, and excitotoxicity and etc. (Ma et al., 2017b; Sweeney et al., 2019; Jing et al., 2020).

Neuroinflammation is a crucial biological process in central nervous system injury that leads to continuous neurological impairment that is characterized by the accumulation of immune cells and the abnormal production of proinflammatory cytokines (O'Brien et al., 2020; Henry and Loane, 2021; Shaheen et al., 2021; Li et al., 2022). Among the proinflammatory cytokines induced by TBI, interleukin (IL)-1 $\beta$  plays a crucial role in triggering the inflammatory cascade and is predominantly regulated by the nucleotide-binding oligomerization domain-like receptor protein 3 (NLRP3) inflammasome (Irrera et al., 2020).

The NLRP3 inflammasome is a multiprotein complex with three protein domains: NACHT, LRR, and PYD domains-containing protein 3 (NLRP3; sensor), apoptosis-associated speck-like protein containing a CARD (ASC; adapter), and caspase-1 (effector) (Sutterwala et al., 2006). When a cell is stimulated by damage-associated molecular pattern molecules, the NLRP3 protein oligomerizes and recruits ASC and procaspase-1, forming the NLRP3 inflammasome, which leads to the activation of procaspase-1 (Ma et al., 2017a; Kelley et al., 2019). Activated caspase-1 cleaves the precursors of IL-1 $\beta$  and IL-18 to form IL-1 $\beta$  and IL-18. IL-1 $\beta$  and IL-18 are the most potent cytokines that initiate inflammation; the increased inflammatory response leads to tissue damage, causing pyroptosis (Jha et al., 2010; Yang et al., 2019b; Chang et al., 2020).

Pyroptosis is an inflammatory form of programmed cell death mediated by caspase-1 activation and IL-1 $\beta$  and IL-18 release (Cookson and Brennan, 2001; Ding et al., 2016). A variety of cell types in multiple central nervous system

diseases can die by pyroptosis, such as microglia, neurons, and astrocytes (de Rivero Vaccari et al., 2014; Gustin et al., 2015; Zhi et al., 2021). Gene knockout or inhibition of key molecules in the pyroptosis pathway, such as NLRP3, absent in melanoma 2, and caspase-1, can inhibit TBI damage and sequelae in animal models (Adamczak et al., 2014; Ge et al., 2018; Liu et al., 2018a).

Sirtuin 2 (*SIRT2*) is an NAD<sup>+</sup>-dependent deacetylase involved in energy metabolism, oxidative stress, inflammation, cell apoptosis, and cell cycle regulation (Harting and Knöll, 2010). The role of *SIRT2* in neurological diseases remains controversial. Some studies have shown that *SIRT2* inhibition or *Sirt2* knockout has a protective effect on neurodegenerative diseases and cerebral ischemia (Xie et al., 2017; Fourcade et al., 2018; Wu et al., 2018), whereas others showed the opposite effect (Eshun-Wilson et al., 2019; Wang et al., 2019). However, few TBI studies have investigated the relationship between *SIRT2* and NLRP3. Therefore, we aimed to investigate whether *SIRT2* can affect the NLRP3 inflammasome, which affects neuroinflammation and pyroptosis of nerve cells in TBI, and to explore mechanisms of action.

According to 2017 statistics from the TBI Model Systems National Database (National Institute on Disability, Independent Living and Rehabilitation Research, U.S. Department of Health and Human Services), cases of TBI in men greatly outnumbered cases in women and accounted for more than 73% of all TBIs reported (Capizzi et al., 2020). Estrogen also has a neuroprotective effect on TBI (Brotfain et al., 2016). Therefore, female mice were excluded from the present study to reduce data variability.

## Methods

### Animals and experimental design

Adult male *Sirt2* knockout mice (*Sirt2*<sup>-/-</sup>, RRID: IMSR\_JAX:012772; 8–10 weeks, 20–25 g; Shanghai Model Organisms Center, Inc., Shanghai, China) and adult male wild type (WT) C57BL/6J mice (8–10 weeks, 20–25 g; Shanghai SLAC Laboratory Animal Corp., Shanghai, China) were used for our *in vivo* study. We also used 12 pregnant *Sirt2*<sup>+/-</sup> mice and 12 pregnant WT C57BL/6J mice. The mice were housed under a standard 12-hour light/dark cycle at 23  $\pm$  2°C

Department of Neurosurgery, Shanghai Jiao Tong University Affiliated Sixth People's Hospital, Shanghai Jiao Tong University, Shanghai, China

\*Correspondence to: Heng-Li Tian, MD, PhD, tianhlsh@126.com.

<https://orcid.org/0000-0003-0525-503X> (Heng-Li Tian)

**Funding:** This work was supported by the National Nature Science Foundation of China, Nos. 81671207 and 81974189 (both to HLT).

**How to cite this article:** Wang W, Gong QY, Cai L, Jing Y, Yang DX, Yuan F, Chen H, Tian HL (2023) Knockout of *Sirt2* alleviates traumatic brain injury in mice. *Neural Regen Res* 18(2):350-356.

with controlled humidity. All experimental procedures were approved by the Institutional Animal Care and Use Committee of Shanghai Sixth People's Hospital affiliated to Shanghai Jiao Tong University, Shanghai, China (approved on March 2, 2016). All experiments were designed and reported according to the Animal Research: Reporting of *In Vivo* Experiments (ARRIVE) guidelines (Percie du Sert et al., 2020). Every necessary effort was taken to minimize the suffering and pain of the mice.

The *Sirt2*<sup>-/-</sup> and WT mice were randomly assigned to four groups: sham-WT, sham-*Sirt2*<sup>-/-</sup>, TBI-WT, and TBI-*Sirt2*<sup>-/-</sup>. A total of 244 mice were used in our study, and the experimental design is given in **Figure 1**. The mice were anesthetized intraperitoneally with xylazine (75 mg/kg; Sigma-Aldrich, St. Louis, MO, USA) and ketamine (10 mg/kg; Aladdin Biochemical Technology Co. Ltd., Shanghai, China) both for operations and for euthanasia in this study.

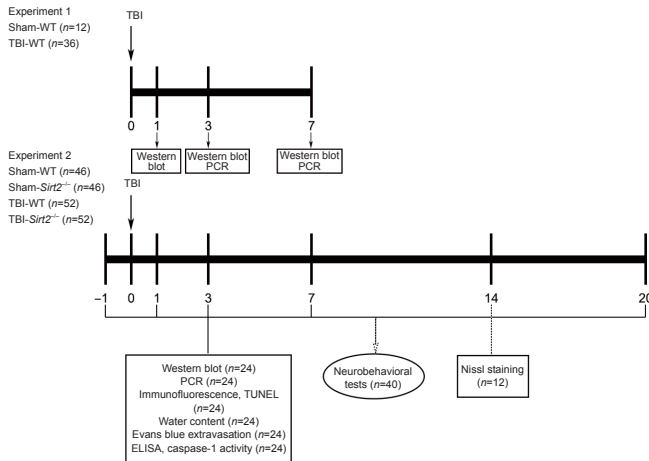


**Figure 1 | Experimental design.**

ELISA: Enzyme-linked immunosorbent assay; PCR: polymerase chain reaction; *Sirt2*: Sirtuin 2; TBI: traumatic brain injury; TUNEL: terminal deoxynucleotidyl transferase dUTP nick-end labeling; WT: wild type.

**Establishment of the TBI model by controlled cortical impact**

The TBI model was established by controlled cortical impact (CCI). Each anesthetized mouse was fixed in place with a stereotactic instrument (Stoelting Co., Wood Dale, IL, USA) and placed on a heat pad to maintain their body temperature at 37°C. A 1-cm incision was made in the middle of the scalp, and the incision was opened bilaterally with retractors. A bone window was made in the center of the right parietal bone using a trephine. Then, a precision cortical impactor (PCI3000, Hatteras Instruments, Inc., Cary, NC, USA) was used to establish TBI. The tip of the impactor was oriented perpendicular to the cortex. The velocity of impact was 1.5 m/s, the deformation depth was 1.5 mm, and the duration was 100 ms. The bone window was then fixed in place with bone wax, and the skin was sutured and disinfected with iodine. Each mouse recovered from anesthesia in a heated cage before being returned to its home cage. In the sham group, no CCI injury was performed after the bone window was opened.

**Cell culture and mechanical stretch injury cell model**

The pregnant *Sirt2*<sup>-/-</sup> and WT C57BL/6J mice were killed by anesthesia to obtain primary cortical neurons from fetal mice (embryonic days 16–18). The skull, meninges, and superficial blood vessels were removed from each fetal mouse, and then the cortex was separated from both hemispheres and cut into pieces. The cortex was gently digested in 0.25% trypsin (Thermo Fisher Scientific, Waltham, MA, USA) at 37°C for 15 minutes, and digestion was terminated with 10% fetal bovine serum (Thermo Fisher Scientific). The cell suspension was mechanically dissociated using 70-µm nylon sieves (BD Biosciences, San Jose, CA, USA). After centrifugation, cells were resuspended in Dulbecco's Modified Eagle Medium (Thermo Fisher Scientific) supplemented with 10% fetal bovine serum. The cells were seeded into poly-D-lysine-coated six-well BioFlex® culture plates (Flexcell International Corp., Burlington, NC, USA) at 1 × 10<sup>5</sup> cells per well. Neurons were cultured in Neurobasal Medium (Thermo Fisher Scientific) with B-27 supplement (Thermo Fisher Scientific), GlutaMAX (Thermo Fisher Scientific), and penicillin and streptomycin (Thermo Fisher Scientific). Cells were cultured for 10–12 days in 5% CO<sub>2</sub> at 37°C under sterile conditions.

Mechanical stretch injury (SI) of primary cortical neurons was used to simulate rotational TBI and was generated using the Cell Injury Controller II system (Custom Design & Fabrication, Inc., Sandston, VA, USA). The control used was a burst of nitrogen of 50-ms duration, which caused 7.5-mm deformation of a silicone rubber membrane (Xu et al., 2017a).

**Neurobehavioral tests**

The modified neurological severity score was used to evaluate neurological deficits (Yang et al., 2019a) before TBI and at 1, 3, 7, and 14 days post-TBI. A score of 0 indicates normal behavior, and a score of 14 indicates maximal neurological deficit.

The rotarod test was used to evaluate the motor coordination of mice (Yang

et al., 2019a). Briefly, each mouse was trained for 3 days with 3 trials per day at 5 minutes per trial. The speed of the rod was accelerated to 40 revolutions/minute. Mice that could not stay on the rod for 5 minutes were excluded from data analysis. The latency for mice that stayed on the rod was recorded before TBI and at 1, 3, 7, and 14 days post-TBI.

The Morris water maze test was used to assess spatial memory (Xu et al., 2018). A pool was divided into four equal quadrants, and a 10-cm-diameter circular platform was placed in a quadrant 1 cm below the water. On days 15–19 post-TBI, each mouse was given 60 seconds to locate the hidden platform. If the mouse failed to find the platform within 60 seconds, it was guided onto the platform and kept on it for 15 seconds. On day 20, the platform was removed and each mouse was placed into the water in the quadrant diagonal to the platform's prior location. The number of crossings at the platform location and the time spent in the target quadrant were recorded.

**Brain water content measurement**

The wet–dry weight method (Yang et al., 2019a) was used to determine brain edema at 3 days post-TBI. Briefly, the mouse brain was removed immediately after euthanasia without heart perfusion, and the ipsilateral injured cerebral tissue was separated and weighed using a precise analytical balance (Mettler Toledo, Columbus, OH, USA) to measure the wet weight. Then, the ipsilateral injured cerebral tissue was dried at 100°C for 72 hours before the dry weight was measured. Brain water content (%) was calculated as follows: (wet weight – dry weight)/wet weight × 100.

**Blood-brain barrier integrity measurement**

BBB integrity was determined by Evans blue (EB) dye extravasation. At 70 hours post-TBI, the mice were anesthetized, and 2% EB (Sigma-Aldrich) was injected intravenously and kept in circulation for 2 hours. The mice were euthanized and then transcardially perfused with normal saline to remove all dye. The brain was removed from each mouse and divided into the two hemispheres. The tissues were immediately weighed, homogenized in 50% trichloroacetic acid (Sigma-Aldrich) solution, and then centrifuged at 12,000 × g for 20 minutes. The supernatant was transferred into a new tube for precipitation with 3 volumes of ethanol. EB extravasation was determined as the optical density at 610 nm using a microplate reader (Agilent Technologies, Santa Clara, CA, USA).

**Nissl and terminal deoxynucleotidyl transferase dUTP nick-end labeling staining**

Samples were collected at 3 days post-operation for terminal deoxynucleotidyl transferase dUTP nick-end labeling (TUNEL) staining and at 14 days post-TBI or post-sham operation for Nissl staining.

Nissl staining was used to determine the brain lesion volume. After euthanasia and transcardial perfusion with normal saline, brain tissues were fixed with 4% paraformaldehyde and sectioned at 4 µm. Sections were stained with Nissl stain, and the lesion volume was calculated using ImageJ (National Institutes of Health, Bethesda, MD, USA) (Schneider et al., 2012).

The TUNEL assay was used to detect pyroptosis. TUNEL staining was performed using the *In Situ* Cell Death Detection Kit (Roche, Basel, Switzerland) in accordance with the manufacturer's instructions. A fluorescence microscope (Leica, Wetzlar, Germany) was used to view and record images. For each mouse, three equally spaced coronal sections were selected from the injury site, and the number of pyroptotic cells was counted in each section in five random fields of view.

**Immunofluorescence staining**

Glial fibrillary acidic protein (GFAP), neuronal nuclei antigen (NeuN), and ionized calcium-binding adapter molecule 1 (Iba-1) were used to identify astrocytes, neurons, and microglia at 3 days post-TBI, respectively. The brain samples were quick-frozen in –80°C isopentane and cut into coronal sections of 30 µm using a freezing microtome (Leica). The cryosections and primary cortical neuron cells were fixed with 4% paraformaldehyde (Beyotime Biotechnology, Shanghai, China). Subsequently, the samples were permeabilized with Triton X-100 (Sigma-Aldrich), blocked with 10% bovine serum albumin (Beijing Solarbio Science & Technology Co., Ltd., Beijing, China) for 1.5 hours, and incubated with the primary antibodies at 4°C overnight as follows: goat anti-CD31 (1:200, R&D Systems, Minneapolis, MN, USA, Cat# AF3628, RRID: AB\_2161028), rabbit anti-zonula occludens 1 (ZO-1; 1:200, Thermo Fisher Scientific, Cat# 61-7300, RRID: AB\_2533938), mouse anti-NeuN (1:200, MilliporeSigma, Burlington, MA, USA, Cat# MAB377, RRID: AB\_2298772), mouse anti-GFAP (1:200, MilliporeSigma, Cat# MAB3402, RRID: AB\_94844), mouse anti-Iba-1 (1:200, Abcam, Cambridge, UK, Cat# ab283319), or rabbit anti-NLRP3 (1:200, Abcam, Cat# ab214185, RRID: AB\_2819003). Then the samples were incubated with the corresponding secondary antibodies for 1 hour at 37°C as follows: donkey anti-goat IgG-Alexa Fluor 555 (1:500, Thermo Fisher Scientific, Cat# A-21432, RRID: AB\_2535853), donkey anti-rabbit IgG-Alexa Fluor 594 (1:500, Thermo Fisher Scientific, Cat# A-21207, RRID: AB\_141637), or donkey anti-mouse IgG-Alexa Fluor 488 (1:500, Thermo Fisher Scientific, Cat# A-21202, RRID: AB\_141607). The samples were incubated with 4',6-diamidino-2-phenylindole dihydrochloride (1:2000, Thermo Fisher Scientific) for 5 minutes at room temperature in the dark. Images were captured with a fluorescence microscope (Leica). Fluorescence intensity was quantified by LAS AF 2.8.0 software (Leica).

**Western blot assay**

Proteins from brain tissue at 3 days post-TBI and primary cortical neurons at

24 hours post-SI were separated by sodium dodecyl sulfate-polyacrylamide gel electrophoresis and transferred to polyvinylidene fluoride membranes. The membranes were blocked with 5% nonfat milk for 1 hour and incubated in primary antibody overnight at 4°C and in the corresponding secondary antibody for 2 hours at room temperature. The antibodies were as follows: rabbit anti-ZO-1 (1:1000, Thermo Fisher Scientific, Cat# 61-7300, RRID: AB\_2533938), rabbit anti-NLRP3 (1:500, Abcam, Cat# ab214185, RRID: AB\_2819003), goat anti-ASC (1:500, Santa Cruz Biotechnology, Dallas, TX, USA, Cat# sc-22514-R, RRID: AB\_2174874), rabbit anti-caspase-1 p45, p10 (1:1000, Cell Signaling Technology, Danvers, MA, USA, Cat# 24232, RRID: AB\_2890194), rabbit-anti-caspase-1 p20 (1:1000, www.antibodies-online.com, Cat# ABIN5675787), mouse anti-β-actin (1:1000, Cell Signaling Technology, Cat# 3700, RRID: AB\_2242334), mouse anti-β-tubulin (1:1000, Cell Signaling Technology, Cat# 86298, RRID: AB\_2715541), anti-mouse IgG-horseradish peroxidase (1:5000, Cell Signaling Technology, Cat# 7076, RRID: AB\_330924), or anti-rabbit IgG-horseradish peroxidase (1:5000, Cell Signaling Technology, Cat# 7074, RRID: AB\_2099233). Protein was visualized using an electrochemiluminescence reagent (Cat# WBKLS0100, MilliporeSigma) and a chemiluminescence instrument (Tanon, Shanghai, China). The relative protein levels were expressed by optical density ratio to β-actin.

#### Real-time reverse transcription-polymerase chain reaction

Total RNA was isolated from primary cultured neurons at 24 hours post-SI or brain tissue at 3 days post-TBI using TRIzol reagent (Thermo Fisher Scientific), and the RNA was reverse transcribed into a complementary DNA template using a PrimeScript™ Reverse Transcription Reagent Kit (Takara Bio, Kyoto, Japan). Real-time reverse transcription-polymerase chain reaction (PCR) was performed using a SYBR Premix Ex Taq Kit (Takara Bio) on an ABI 7900HT PCR instrument (Thermo Fisher Scientific). The following primers were used: NLRP3 (forward: 5'-ATC AAC AGG CAG CTC TG-3' and reverse: 5'-GTC CTC CTG CAT ACC ATA GA-3'), ASC (forward: 5'-GAC AGT GCA ACT GGC GAG AAG-3' and reverse: 5'-CGA CTC CAG ATA GTA GGC TGA C-3'), caspase-1 (forward: 5'-ACA AGG CAC GGA CCT ATG-3' and reverse: 5'-TCC CAG TCA GTC CTG GAA ATG-3'), IL-1β (forward: 5'-GCA ACT GCT CCT GAA CTC AAC T-3' and reverse: 5'-ATC TTT GGG GTC CGT CAA CT-3'), IL-18 (forward: 5'-GAC TCT TGC AAC TTC AAG G-3' and reverse: 5'-CAG GCT GTC TTT TGT CAA CGA-3'), and glyceraldehyde 3-phosphate dehydrogenase (forward: 5'-AGG TCG GTG TGA ACG GAT TTG-3' and reverse: 5'-TGT AGA CCA TTA GTT GAG TCA-3'). Reverse transcription conditions were as follows: predenaturation at 95°C for 30 seconds, followed by denaturation at 95°C for 5 seconds and annealing and extension at 60°C for 30 seconds, for a total of 40 cycles. We used the comparative Ct (threshold cycle) method (Zhu et al., 2019) normalized to glyceraldehyde 3-phosphate dehydrogenase to analyze relative changes in gene expression.

#### Lactate dehydrogenase assay

The lactate dehydrogenase (LDH) detection kit (Roche) was used to evaluate cell membrane integrity. The primary neurons at 24 hours post-SI were cultured in six-well BioFlex® culture plates (Flexcell International Corp.). The amount of LDH released into the culture medium is represented as LDH activity. The optical density was read at 490 nm with a spectrophotometer (BioTek).

#### Caspase-1 activity measurement

A caspase-1 activity assay kit (Beyotime Biotechnology) was used to measure caspase-1 activity at 3 days post-TBI in accordance with the manufacturer's instructions (Liu et al., 2018a). Briefly, brain tissues were lysed, and the supernatant was collected. A standard curve was prepared using a p-nitroaniline standard. Then, the optical density of the tissue lysates was read at 405 nm on a microplate reader (BioTek).

#### Enzyme-linked immunosorbent assay

An enzyme-linked immunosorbent assay (ELISA) kit (Beijing Solarbio Science & Technology Co., Ltd.) was used to measure the level of IL-1β in accordance with the manufacturer's instructions. Mouse blood samples were collected using retro-orbital bleeding at 3 days post-TBI, centrifuged, and the supernatant was collected. Then the samples were added for 90 minutes to an ELISA plate coated with IL-1β antibody. After washing, the plate was sequentially treated with biotinylated IL-1β antibody, horseradish peroxidase-labeled streptavidin, and 3,3',5,5'-tetramethylbenzidine. The optical density of the samples was read on a microplate reader (BioTek) at 450 nm.

#### Statistical analysis

No statistical methods were used to predetermine sample sizes; however, our sample sizes are similar to those reported in previous publications (Xu et al., 2017a, b). No animals or data points were excluded from the analysis. The evaluators were blinded to the assignment. All data were indicated as mean ± standard deviation. The comparisons between two groups were performed by Student's t-test.  $P < 0.05$  was considered statistically significant. SPSS (Version 21.0, IBM, Armonk, NY, USA) and GraphPad Prism 5.01 for Windows (GraphPad Software, San Diego, CA, USA, www.graphpad.com) were used for statistical analysis and visualization, respectively.

## Results

### The NLRP3 inflammasome is upregulated in the pericontusional area post-TBI

Western blot and PCR were performed to examine the NLRP3, ASC, and caspase-1 protein and mRNA levels, respectively, in pericontusional regions of WT mice at different time points post-TBI. The protein and mRNA expression levels of NLRP3, ASC, and caspase-1 all increased post-TBI; this increase

peaked on day 3 and lasted at least 7 days (Figure 2A–G). Therefore, we selected WT mouse brain slices 3 days post-TBI to detect NLRP3 expression in neurons, astrocytes, and microglia using the immunofluorescence method. The results indicated that NLRP3 was expressed in neurons and microglia post-TBI (Figure 2H).

### Knockout of *Sirt2* improves neurological function post-TBI in mice

There was no neurological deficit in WT or *Sirt2*<sup>-/-</sup> mice after the sham operation. After TBI, the modified neurological severity scores increased significantly on day 1 in both groups of mice; the scores significantly reduced on days 3, 7, and 14 in *Sirt2*<sup>-/-</sup> mice compared with those in WT mice ( $P < 0.05$ ; Figure 3A). The *Sirt2*<sup>-/-</sup> mice had longer latency than WT mice on the rotarod test on days 7 and 14 post-TBI ( $P < 0.05$ ; Figure 3B). In the Morris water maze test, the *Sirt2*<sup>-/-</sup> mice had a greater number of crossings at the platform location and stayed longer in the target quadrant on day 20 post-TBI compared with WT mice ( $P < 0.01$ ; Figure 3C–E).

### Knockout of *Sirt2* alleviates blood-brain barrier disruption and brain edema in mice after traumatic brain injury

TBI leads to BBB disruption. ZO-1 is a fundamental constituent of the BBB and plays a crucial role in maintaining BBB integrity (Cash and Theus, 2020). Immunostaining of brain tissues at 3 days post-TBI for ZO-1 and the vascular marker CD31 showed continuous costaining of ZO-1 and CD31 in the sham group, consistent with previous results (Xu et al., 2017b). ZO-1 gaps were present post-TBI, with fewer gaps in the TBI-*Sirt2*<sup>-/-</sup> group than in the TBI-WT group (Figure 4A). Meanwhile, western blot analysis revealed a much higher expression level of ZO-1 in the TBI-*Sirt2*<sup>-/-</sup> group than in the TBI-WT group at 3 days post-TBI ( $P < 0.05$ ; Figure 4B and C).

Nissl staining was used to calculate the volume of damaged brain tissue post-TBI in mice. The TBI-*Sirt2*<sup>-/-</sup> group had significantly reduced volume of damaged tissue post-TBI compared with the TBI-WT group ( $P < 0.05$ ; Figure 4D and E).

EB extravasation and brain water content were used to estimate BBB integrity post-TBI. *Sirt2*<sup>-/-</sup> mice had significantly decreased EB leakage in the ipsilateral cortex 3 days post-TBI compared with the WT mice post-TBI, indicating that BBB disruption induced by TBI was attenuated by knockout of *Sirt2* ( $P < 0.01$ ; Figure 4F and G). The dry-wet weight results showed that the water content of the injured hemisphere increased post-TBI, and *Sirt2*<sup>-/-</sup> mice had significantly reduced brain water content compared with the WT mice post-TBI ( $P < 0.01$ ; Figure 4H).

### Knockout of *Sirt2* reduces the levels of NLRP3 inflammasome and nerve cell pyroptosis after traumatic brain injury

Western blot and PCR were used to detect the protein and mRNA expression levels, respectively, of each component in the NLRP3 inflammasome on day 3 post-TBI. The protein expression levels of NLRP3, ASC, and caspase-1 were increased in WT mice post-TBI compared with the sham-treated mice. The protein expression levels of NLRP3, ASC, and caspase-1 were significantly decreased in the *Sirt2*<sup>-/-</sup> mice at 3 days post-TBI compared with the WT mice (all  $P < 0.05$ ; Figure 5A–F). The protein expression levels were consistent with the mRNA levels (Figure 5G–I).

Neuroinflammation is mediated by inflammatory cells and the cytokines secreted by the inflammatory cells (O'Brien et al., 2020). We used PCR to detect the mRNA expression levels of IL-1β and IL-18 in the brain tissue around the lesion 3 days post-TBI, and we used ELISA to detect the protein expression levels of IL-1β in blood 3 days post-TBI. The PCR results showed that *Sirt2*<sup>-/-</sup> mice had significantly reduced IL-1β and IL-18 mRNA levels post-TBI compared with WT mice ( $P < 0.01$ ; Figure 5J). ELISA results also showed that *Sirt2*<sup>-/-</sup> mice had significantly reduced secretion of IL-1β in the blood compared with WT mice ( $P < 0.01$ ; Figure 5K).

Caspase-1 is an effector of the NLRP3 inflammasome, and caspase-1 activity determines the inflammatory response mediated by the NLRP3 inflammasome (Miao et al., 2011). We found that caspase-1 activity was significantly elevated in the brain tissues post-TBI, and its activity was increased less in *Sirt2*<sup>-/-</sup> mice than in WT mice on day 3 post-TBI ( $P < 0.01$ ; Figure 5L).

We used TUNEL staining to detect DNA damage in nerve cells of brain tissue at 3 days post-TBI. The results showed very few TUNEL-positive cells in the sham group, but many TUNEL-positive cells were present 3 days post-TBI. Furthermore, *Sirt2*<sup>-/-</sup> mice had significantly reduced numbers of TUNEL-positive cells compared with WT mice post-TBI ( $P < 0.01$ ; Figure 5M and N).

### *Sirt2* knockout reduces NLRP3 inflammasome expression and primary neuron pyroptosis after mechanical stretch injury

We used primary cultured neurons to investigate the underlying mechanism of *Sirt2* knockout post-SI *in vitro*. Western blot analysis showed that the protein expression levels of NLRP3 ( $P < 0.05$ ), ASC ( $P < 0.01$ ), and caspase-1 ( $P < 0.01$ ) were significantly decreased in the SI-*Sirt2*<sup>-/-</sup> group compared with those in the SI-WT group (Figure 6A–F), which were similar to our *in vivo* results.

LDH release tests are used to assess cell membrane integrity. Cytoplasmic LDH is released into the culture medium when the cell membrane integrity is compromised (Jing et al., 2020). Compared with the control group without intervention, LDH dramatically increased after SI, while knockout of *Sirt2* reduced the release of LDH from primary neurons induced by SI ( $P < 0.01$ ; Figure 6G). The numbers of TUNEL-positive primary neuron cells were significantly reduced in the SI-*Sirt2*<sup>-/-</sup> group compared with those in the SI-WT group ( $P < 0.01$ ; Figure 6H and I).

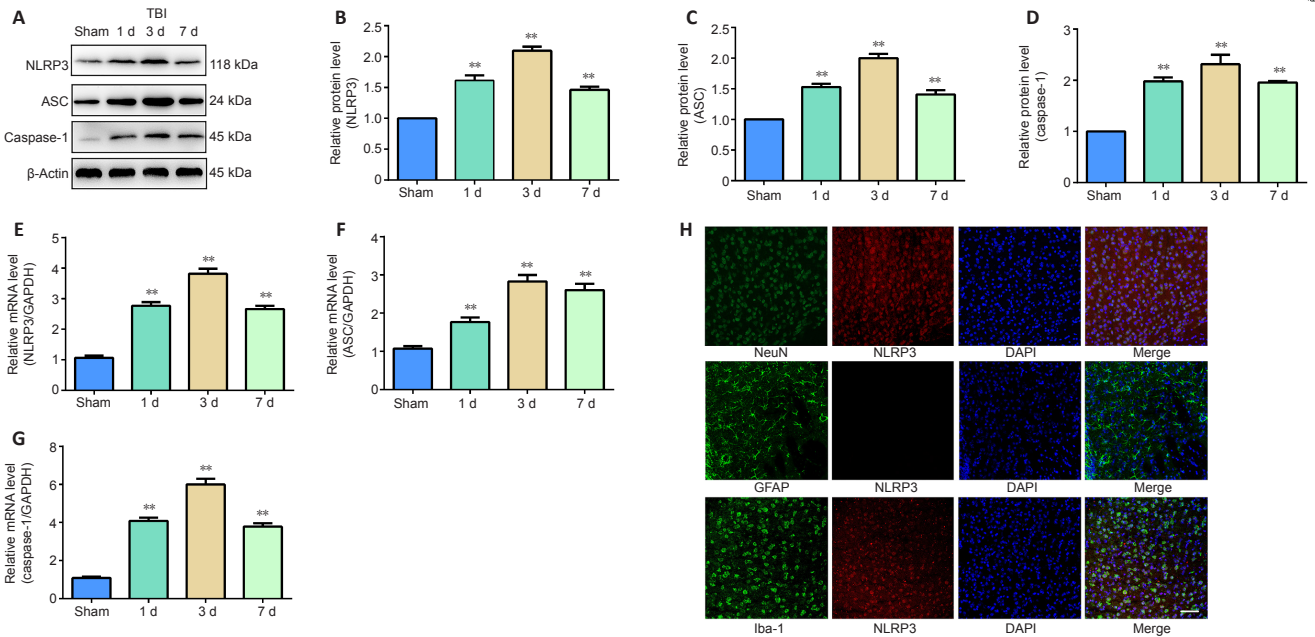


**Figure 2 | The NLRP3 inflammasome is upregulated in the pericontusional area of wild type mice after traumatic brain injury.** (A) Western blot bands of the NLRP3 inflammasome in the pericontusional area. (B–D) Quantification of NLRP3, ASC, and caspase-1 protein expression, normalized to the sham group. (E–G) Quantification of NLRP3, ASC, and caspase-1 relative mRNA levels by PCR. Data are expressed as mean ± SD (n = 6 per group). \*\*P < 0.01, vs. sham group (Student’s t-test). (H) Immunofluorescence staining of NLRP3 expression (red, stained with Alexa Fluor 594) in neurons (NeuN-positive cells, green, stained with Alexa Fluor 488), astrocytes (GFAP-positive cells, green, stained with Alexa Fluor 488), and microglia (Iba-1-positive cells, green, stained with Alexa Fluor 488) at 3 days post-TBI. Scale bar: 50 μm. ASC: Apoptosis-associated speck-like protein containing CARD; DAPI: 4',6-diamidino-2'-phenylindole, dihydrochloride; GAPDH: glyceraldehyde 3-phosphate dehydrogenase; GFAP: glial fibrillary acidic protein; Iba-1: ionized calcium binding adaptor molecule-1; NeuN: neuronal nuclei; NLRP3: nucleotide binding oligomerization domain-like receptor protein 3; PCR: polymerase chain reaction; TBI: traumatic brain injury.

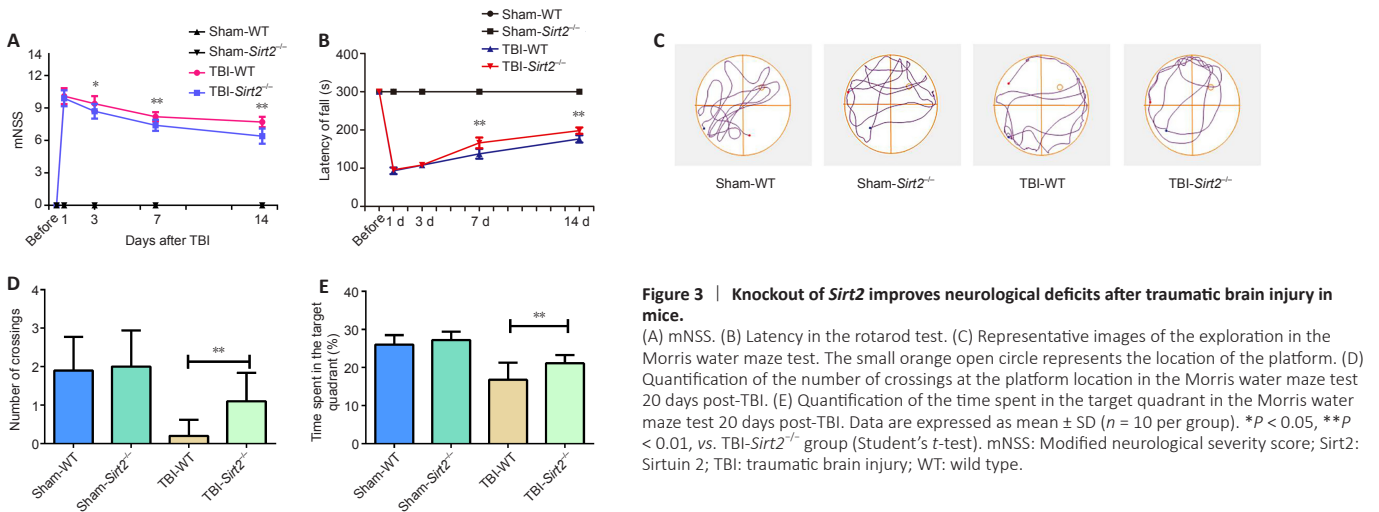


**Figure 3 | Knockout of *Sirt2* improves neurological deficits after traumatic brain injury in mice.** (A) mNSS. (B) Latency in the rotarod test. (C) Representative images of the exploration in the Morris water maze test. The small orange open circle represents the location of the platform. (D) Quantification of the number of crossings at the platform location in the Morris water maze test 20 days post-TBI. (E) Quantification of the time spent in the target quadrant in the Morris water maze test 20 days post-TBI. Data are expressed as mean ± SD (n = 10 per group). \*P < 0.05, \*\*P < 0.01, vs. TBI-Sirt2<sup>-/-</sup> group (Student’s t-test). mNSS: Modified neurological severity score; Sirt2: Sirtuin 2; TBI: traumatic brain injury; WT: wild type.

Discussion

This study demonstrates that *Sirt2* knockout reduces the expression of the components of the NLRP3 inflammasome and the activity of caspase-1, which alleviates neuroinflammation and reduces pyroptosis, leading to reversal of neurological dysfunction and reductions in cerebral edema and BBB disruption.

Secondary injury post-TBI is a gradual process that causes chemical and metabolic changes in nerve cells and leads to a series of pathological changes, such as apoptosis, neuroinflammation, and BBB disruption (Kulbe and Hall, 2017). The processes behind these pathological changes may be vital targets for TBI therapy (Jha et al., 2019). The BBB maintains brain homeostasis by transporting nutrients, removing toxic substances, and inhibiting the entry of peripheral immune cells. The BBB is composed of specialized endothelial cells closely joined by tight junction proteins. The loss of tight junction proteins, such as ZO-1 and occludin, allows typically restricted molecules, such as peripheral immune cells, to pass through the BBB, leading to vasogenic brain edema (Wang et al., 2018). We found that *Sirt2* knockout reduced EB extravasation and brain edema, indicating that *Sirt2* knockout partially reversed the BBB disruption induced by TBI. Furthermore, the results of ZO-1

immunofluorescence staining and western blot analysis showed that *Sirt2* knockout reduced the loss of the tight junction protein ZO-1. Therefore, we hypothesize that SIRT2 improves the integrity of the BBB by reducing the loss of tight junction proteins, thereby alleviating cerebral edema.

Widely used TBI animal models can be generated by fluid percussion injury, CCI injury, weight drop impact injury, blast injury, or penetrating ballistic-like injury (Xiong et al., 2013). We chose to use the CCI model, as it is easy to control the mechanical factors, such as time, speed, and impact depth (Saatman et al., 2006), and it has a wide range of simulation scenarios. We used the parameters of the moderate-TBI CCI model (Liu et al., 2018b).

When pyroptosis occurs, the cells swell, pores are formed in the cell membrane, and the integrity of the cell membrane is lost. The resultant release of IL-1β and IL-18 causes an inflammatory response (Cookson and Brennan, 2001; Ding et al., 2016). Pyroptosis is driven by canonical and noncanonical inflammasomes. In the canonical pathway, the caspase-1 precursor combines with NLRP3 protein and adapter protein ASC to form the NLRP3 inflammasome, which activates caspase-1 and cleaves and activates IL-1β and IL-18 precursors; IL-1β and IL-18 then cleave gasdermin D, which causes formation of holes in the cell membrane, causing cell pyroptosis (Kovacs and Miao, 2017; Sun et al., 2020).

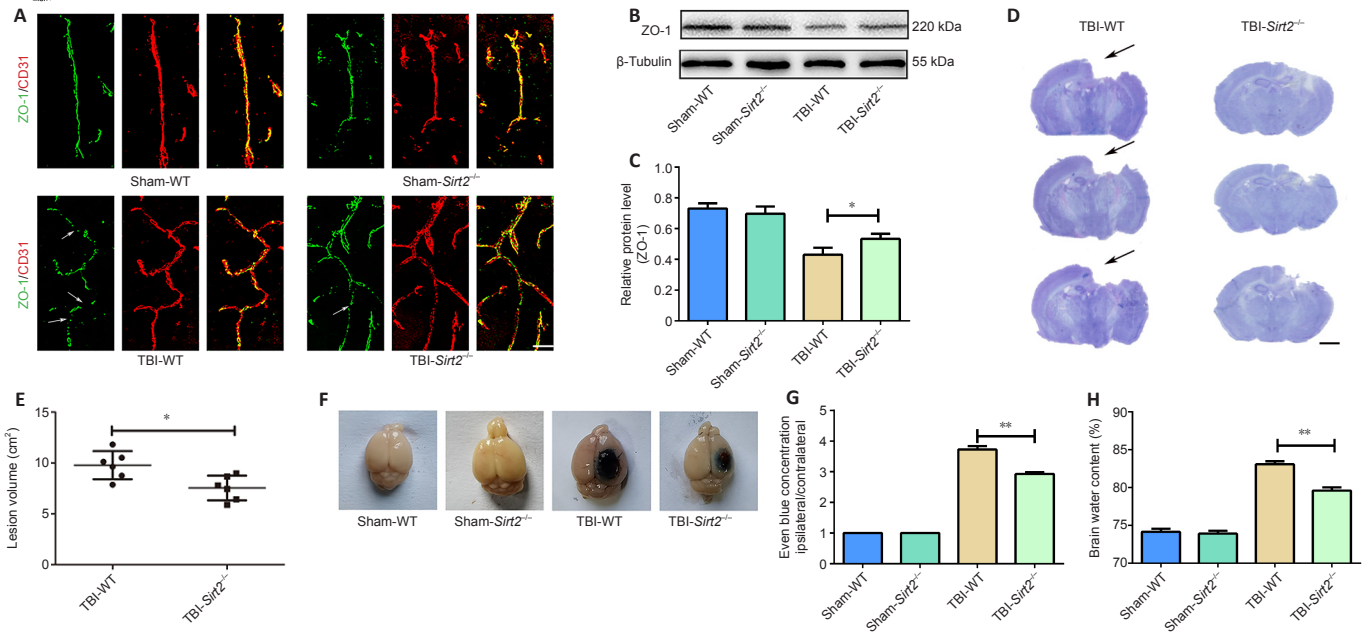


**Figure 4 | Knockout of *Sirt2* alleviates blood-brain barrier disruption and brain edema in mice after traumatic brain injury.** (A) Representative contained immunofluorescence images of ZO-1 (green, stained with Alexa Fluor 488) and CD31 (red, stained with Alexa Fluor 555) at 3 days post-TBI. ZO-1 gaps are indicated by arrows. Scale bar: 10  $\mu$ m. (B) Representative western blot bands of ZO-1 at 3 days post-TBI. (C) Quantification of ZO-1 protein expression normalized to  $\beta$ -tubulin. (D) Representative images of Nissl staining of brain tissue of mice 14 days post-TBI. Scale bar: 3 mm. (E) Quantification of brain lesion volume. (F) Representative images of the amount of Evans blue dye exudation at 3 days post-TBI. (G) Quantification of the amount of Evans blue dye exudation at 3 days post-TBI. (H) Quantification of brain water content. Data are expressed as mean  $\pm$  SD ( $n = 6$  per group). \* $P < 0.05$ , \*\* $P < 0.01$  (Student's *t*-test). *Sirt2*: Sirtuin 2; TBI: traumatic brain injury; WT: wild type; ZO-1: zonula occludens-1.

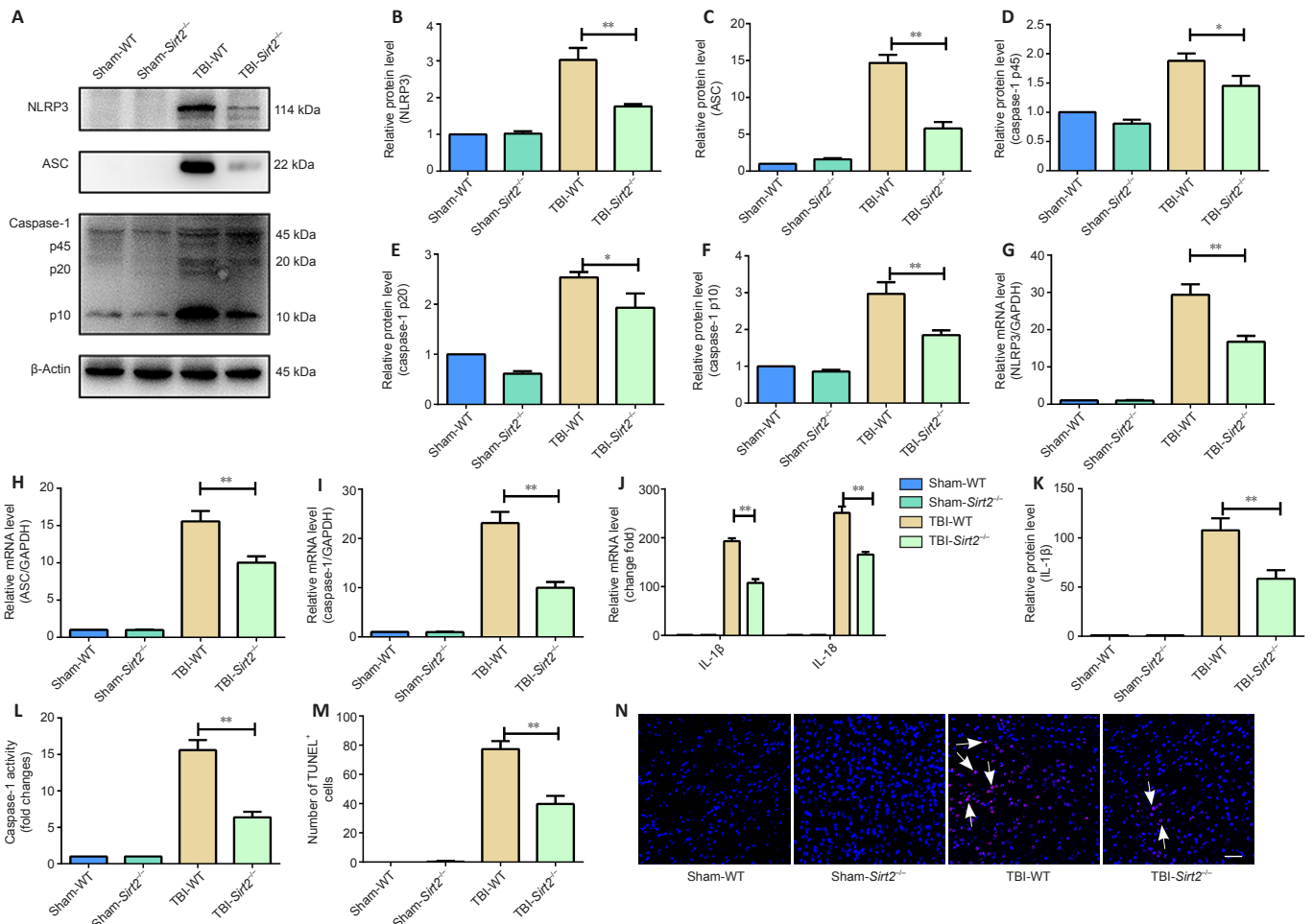


**Figure 5 | Knockout of *Sirt2* reduces the expression of the NLRP3 inflammasome and nerve cell pyroptosis after traumatic brain injury *in vivo*.** (A) Representative western blot bands of the NLRP3 inflammasome components at 3 days post-TBI. (B–F) Quantification of protein expression of NLRP3, ASC, caspase-1 p45, caspase-1 p20, and caspase-1 p10 at 3 days post-TBI. The target protein expression was normalized to the sham-WT group. (G–J) Quantification of mRNA expression of NLRP3, ASC, caspase-1, IL-1 $\beta$ , and IL-18 at 3 days post-TBI by PCR. The target mRNA expression was normalized to the sham-WT group. (K) IL-1 $\beta$  secretion in blood by ELISA. (L) Caspase-1 activity at 3 days post-TBI. (M, N) Representative images and quantification of TUNEL-positive cells (red) at 3 days post-TBI. Double-positive TUNEL (red) and DAPI staining (blue) indicates the pyroptotic cells. Scale bar: 50  $\mu$ m. Data are expressed as mean  $\pm$  SD ( $n = 6$  per group). \* $P < 0.05$ , \*\* $P < 0.01$  (Student's *t*-test). ASC: Apoptosis-associated speck-like protein containing CARD; DAPI: 4',6-diamidino-2-phenylindole; ELISA: enzyme-linked immunosorbent assay; IL: interleukin; NLRP3: nucleotide binding oligomerization domain-like receptor protein 3; PCR: polymerase chain reaction; *Sirt2*: Sirtuin 2; TBI: traumatic brain injury; TUNEL: terminal deoxynucleotidyl transferase-mediated dUTP-biotin nick end labeling; WT: wild type.

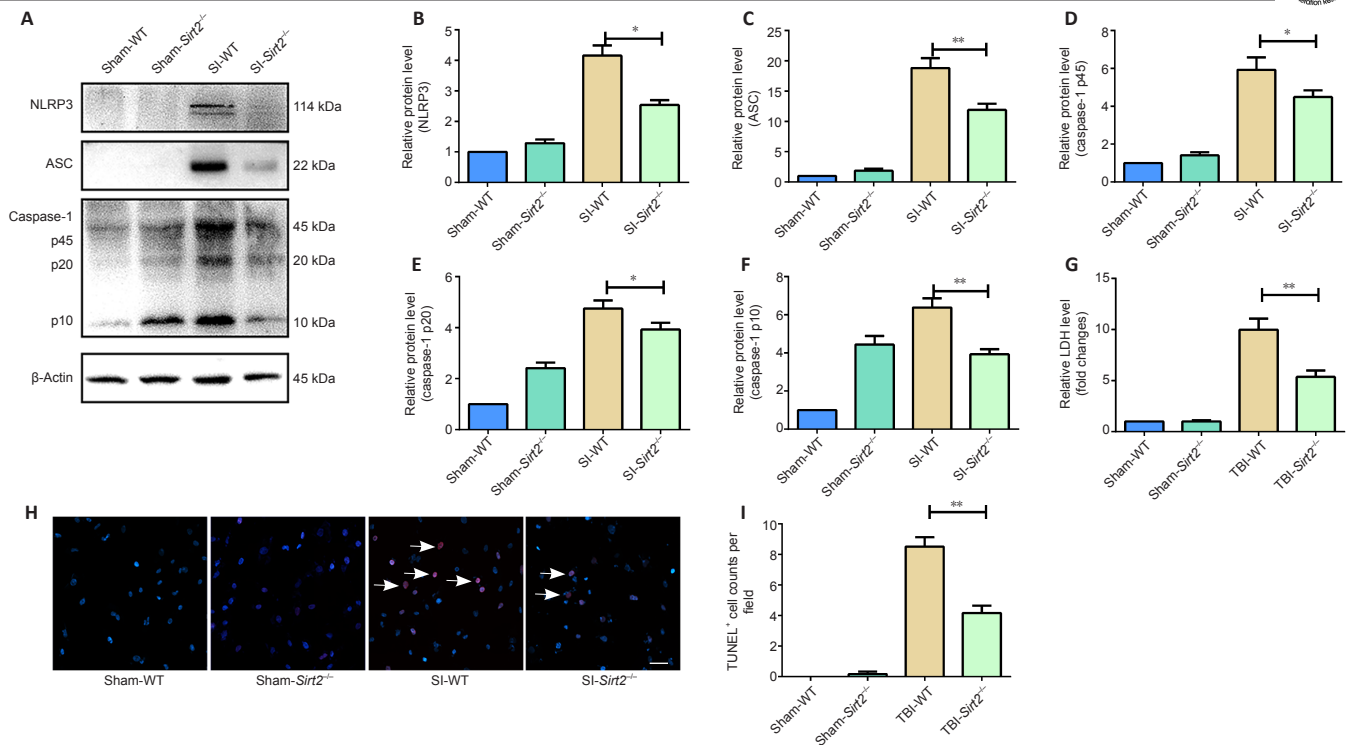


**Figure 6 | Knockout of *Sirt2* reduces NLRP3 inflammasome expression and primary neuron pyroptosis after mechanical stretch injury.** (A) Representative western blot bands of the NLRP3 inflammasome components at 24 hours post-SI. (B–F) Quantification of protein expression of NLRP3, ASC, caspase-1 p45, caspase-1 p20, and caspase-1 p10 at 24 hours post-SI. The target protein expression was normalized to the sham-WT group. (G) Release of LDH from primary neurons induced by SI at 24 hours. (H, I) Representative images and quantification of TUNEL-positive cells (red, arrow) at 24 hours post-SI. Scale bar: 30  $\mu$ m. Data are expressed as mean  $\pm$  SD. Each experiment was repeated three times. \* $P < 0.05$ , \*\* $P < 0.01$  (Student's *t*-test). ASC: apoptosis-associated speck-like protein containing CARD; LDH: lactate dehydrogenase; NLRP3: nucleotide binding oligomerization domain-like receptor protein 3; SI: stretch injury; *Sirt2*: Sirtuin 2; TBI: traumatic brain injury; TUNEL: terminal deoxynucleotidyl transferase dUTP nick-end labeling; WT: wild type.

The role of the NLRP3 inflammasome post-TBI has been confirmed in experimental TBI models and patients with moderate or severe TBI. Liu et al. (2013) reported that NLRP3, ASC, and caspase-1 mRNA increased 6 hours after fluid percussion injury in rats, and the protein levels of NLRP3 and caspase-1 remained increased 24 hours after injury. Chen et al. (2019) showed that NLRP3 mRNA began to increase within 6 hours after TBI and exhibited peaks at 24 and 72 hours post-TBI in mice; on day 7, the expression of NLRP3 decreased to a level that remained higher than the control group. TBI can activate the NLRP3 inflammasome, so we hypothesized that targeting this pathway may effectively alleviate neuroinflammation and promote the recovery from TBI. In animal models of other neuroinflammatory diseases, such as Alzheimer's disease, NLRP3 knockout has been shown to reduce neuroinflammation and improve functional prognosis (Feng et al., 2020). MCC950 is a highly selective and potent NLRP3 inhibitor. A study found that intraperitoneal injection of MCC950 in mice reduced the expression of NLRP3, caspase-1, ASC, and IL-1 $\beta$  24 hours after CCI and decreased IL-1 $\beta$  levels 72 hours post-TBI (Ismael et al., 2018). In our study, expression of the components of the NLRP3 inflammasome increased post-TBI, peaked on day 3, and lasted at least 7 days; these components were expressed in neurons and microglia 3 days post-TBI.

Caspase-1 activity determines the inflammatory response mediated by the NLRP3 inflammasome. Caspase-1 knockout mice are partially resistant to stroke, and intracerebroventricular administration of caspase-1 inhibitors provides protective effects in experimental stroke models (Ross et al., 2007). A study showed that caspase-1 and ASC levels were elevated in the serum of patients post-TBI and were related to poor prognosis post-TBI (Kerr et al., 2018). Sun et al. (2020) demonstrated that VX765, a caspase-1 inhibitor, inhibits IL-1 $\beta$  and IL-18 production, which decreases pyroptosis in the TBI acute phase, decreases LDH release, reduces neuroinflammation, and inhibits microglial death. Thus, the NLRP3 inflammasome plays a key role in regulating neuroinflammation and pyroptosis. Activation of the NLRP3 inflammasome is a two-step process of priming and activation (Swanson et al., 2019). Priming upregulates the expression of the NLRP3 inflammasome and is induced by various signals, such as damage-associated molecular patterns, Toll-like receptors, and tumor necrosis factor, that result in nuclear factor- $\kappa$ B activation (Bauernfeind et al., 2009; Xing et al., 2017). In our study, *Sirt2*<sup>-/-</sup> mice post-TBI had decreased expression of the NLRP3 inflammasome components and decreased caspase-1 activity. We suggest that knockout of *Sirt2* may alleviate neuroinflammation and reduce pyroptosis via the NLRP3/caspase-1 pathway.

The role of SIRT2 in neurological diseases is still controversial. The Parkinson's disease (PD) model generated by long-term administration of 1-methyl-4-phenyl-1,2,3,6-tetrahydropyridine can replicate most of the clinical features of PD and produce reliable and reproducible PD. The SIRT2 inhibitor AK7 can prevent dopamine depletion and dopaminergic neuron loss caused

by 1-methyl-4-phenyl-1,2,3,6-tetrahydropyridine *in vivo* (Chopra et al., 2012). *Sirt2*<sup>-/-</sup> mice had reduced neurodegeneration caused by long-term administration of 1-methyl-4-phenyl-1,2,3,6-tetrahydropyridine, which was caused by a reduction in apoptosis by an increase in FOXO3a acetylation and a reduction in Bcl-2-like protein 11 levels (Liu et al., 2014). In contrast, in the PD model induced by 6-hydroxydopamine treatment, the decrease in SIRT2 activity lead to an increase in acetylated  $\alpha$ -tubulin, and the function of tubulin deacetylase was improved (Patel and Chu, 2014). AK7 treatment can improve motor function, prolong survival, reduce brain atrophy, and significantly reduce the accumulation of mutant huntingtin protein and improve Huntington's disease symptoms (Chopra et al., 2012); however, another study reached the opposite conclusion (Capizzi et al., 2020). *Sirt2* knockout or use of the SIRT2 inhibitor AGK2 showed neuroprotection against cerebral ischemia (Wang et al., 2016). Another study showed that SIRT2 determines the level of  $\alpha$ -tubulin acetylation, which regulates microtubule assembly. Acetylated  $\alpha$ -tubulins are necessary for the activation of the NLRP3 inflammasome (Misawa et al., 2013). Thus, the relationship between SIRT2 and NLRP3 in TBI needs to be further investigated.

There are several limitations to this study. First, the role of SIRT2 in microglial cells was not investigated. Second, we did not use overexpression technology or rescue experiments to validate our hypothesis. Thus, further research needs to be performed. In future studies, we plan to investigate gender differences in the response to *Sirt2* knockout post-TBI.

In conclusion, *Sirt2* knockout can improve the neurological dysfunction of mice post-TBI, improve memory, reduce the loss of tight junction proteins, reduce the disruption of the BBB, and reduce cerebral edema. *Sirt2* knockout may reduce neuroinflammation and pyroptosis by reducing the expression of the NLRP3 inflammasome and the activity of caspase-1.

**Author contributions:** Study design: WW, HLT; manuscript writing: WW. All authors participated in experiment implementation, analyzed data, and approved the final version of manuscript for publication.

**Conflicts of interest:** No competing financial interests exist.

**Availability of data and materials:** All data generated or analyzed during this study are included in this published article and its supplementary information files.

**Open access statement:** This is an open access journal, and articles are distributed under the terms of the Creative Commons AttributionNonCommercial-ShareAlike 4.0 License, which allows others to remix, tweak, and build upon the work non-commercially, as long as appropriate credit is given and the new creations are licensed under the identical terms.

**Open peer reviewers:** *Chao Weng, Renmin Hospital of Wuhan University, China; Fei Ding, Affiliated Hospital of Nantong University, China; Rosario Donato, Interuniversity Institute of Myology, Italy.*

**Additional file:** *Open peer review reports 1–3.*

## References

- Adamczak SE, de Rivero Vaccari JP, Dale G, Brand FJ, 3rd, Nonner D, Bullock MR, Dahl GP, Dietrich WD, Keane RW (2014) Pyroptotic neuronal cell death mediated by the AIM2 inflammasome. *J Cereb Blood Flow Metab* 34:621-629.
- Bauernfeind FG, Horvath G, Stutz A, Alnemri ES, MacDonald K, Speert D, Fernandes-Alnemri T, Wu J, Monks BG, Fitzgerald KA, Hornung V, Latz E (2009) Cutting edge: NF-kappaB activating pattern recognition and cytokine receptors license NLRP3 inflammasome activation by regulating NLRP3 expression. *J Immunol* 183:787-791.
- Brotfain E, Gruenbaum SE, Boyko M, Kutz R, Zlotnik A, Klein M (2016) Neuroprotection by estrogen and progesterone in traumatic brain injury and spinal cord injury. *Curr Neuropharmacol* 14:641-653.
- Capizzi A, Woo J, Verdusco-Gutierrez M (2020) Traumatic brain injury: an overview of epidemiology, pathophysiology, and medical management. *Med Clin North Am* 104:213-238.
- Cash A, Theus MH (2020) Mechanisms of blood-brain barrier dysfunction in traumatic brain injury. *Int J Mol Sci* 21:3344.
- Chang Y, Zhu J, Wang D, Li H, He Y, Liu K, Wang X, Peng Y, Pan S, Huang K (2020) NLRP3 inflammasome-mediated microglial pyroptosis is critically involved in the development of post-cardiac arrest brain injury. *J Neuroinflammation* 17:219.
- Chen Y, Meng J, Xu Q, Long T, Bi F, Chang C, Liu W (2019) Rapamycin improves the neuroprotection effect of inhibition of NLRP3 inflammasome activation after TBI. *Brain Res* 1710:163-172.
- Chopra V, Quinti L, Kim J, Voller L, Narayanan KL, Edgerly C, Cipicchio PM, Lauver MA, Choi SH, Silverman RB, Ferrante RJ, Hersch S, Kazantsev AG (2012) The sirtuin 2 inhibitor AK-7 is neuroprotective in Huntington's disease mouse models. *Cell Rep* 2:1492-1497.
- Cookson BT, Brennan MA (2001) Pro-inflammatory programmed cell death. *Trends Microbiol* 9:113-114.
- de Rivero Vaccari JP, Dietrich WD, Keane RW (2014) Activation and regulation of cellular inflammasomes: gaps in our knowledge for central nervous system injury. *J Cereb Blood Flow Metab* 34:369-375.
- Ding J, Wang K, Liu W, She Y, Sun Q, Shi J, Sun H, Wang DC, Shao F (2016) Pore-forming activity and structural autoinhibition of the gasdermin family. *Nature* 535:111-116.
- Eshun-Wilson L, Zhang R, Portran D, Nachury MV, Toso DB, Lohr T, Vendruscolo M, Bonomi M, Fraser JS, Nogales E (2019) Effects of  $\alpha$ -tubulin acetylation on microtubule structure and stability. *Proc Natl Acad Sci U S A* 116:10366-10371.
- Feng YS, Tan ZX, Wu LY, Dong F, Zhang F (2020) The involvement of NLRP3 inflammasome in the treatment of Alzheimer's disease. *Ageing Res Rev* 64:101192.
- Fourcade S, Outeiro TF, Pujol A (2018) SIRT2 in age-related neurodegenerative disorders. *Ageing (Albany N Y)* 10:295-296.
- Ge X, Li W, Huang S, Yin Z, Xu X, Chen F, Kong X, Wang H, Zhang J, Lei P (2018) The pathological role of NLRs and AIM2 inflammasome-mediated pyroptosis in damaged blood-brain barrier after traumatic brain injury. *Brain Res* 1697:10-20.
- Gustin A, Kirchmeyer M, Koncina E, Felten P, Losciuto S, Heurtaux T, Tardivel A, Heuschling P, Dostert C (2015) NLRP3 inflammasome is expressed and functional in mouse brain microglia but not in astrocytes. *PLoS One* 10:e0130624.
- Harting K, Knöll B (2010) SIRT2-mediated protein deacetylation: An emerging key regulator in brain physiology and pathology. *Eur J Cell Biol* 89:262-269.
- Henry RJ, Loane DJ (2021) Targeting chronic and evolving neuroinflammation following traumatic brain injury to improve long-term outcomes: insights from microglial-depletion models. *Neural Regen Res* 165:976-977.
- Irrera N, Russo M, Pallio G, Bitto A, Mannino F, Minutoli L, Altavilla D, Squadrito F (2020) The role of NLRP3 inflammasome in the pathogenesis of traumatic brain injury. *Int J Mol Sci* 21:6204.
- Ismael S, Nasoohi S, Ishrat T (2018) MCC950, the selective inhibitor of nucleotide oligomerization domain-like receptor protein-3 inflammasome, protects mice against traumatic brain injury. *J Neurotrauma* 35:1294-1303.
- Jha RM, Kochanek PM, Simard JM (2019) Pathophysiology and treatment of cerebral edema in traumatic brain injury. *Neuropharmacology* 145:230-246.
- Jha S, Srivastava SY, Brickey WJ, Iocca H, Toews A, Morrison JP, Chen VS, Gris D, Matsushima GK, Ting JP (2010) The inflammasome sensor, NLRP3, regulates CNS inflammation and demyelination via caspase-1 and interleukin-18. *J Neurosci* 30:15811-15820.
- Jing Y, Yang DX, Wang W, Yuan F, Chen H, Ding J, Geng Z, Tian HL (2020) Aloin protects against blood-brain barrier damage after traumatic brain injury in mice. *Neurosci Bull* 36:625-638.
- Kelley N, Jeltema D, Duan Y, He Y (2019) The NLRP3 inflammasome: an overview of mechanisms of activation and regulation. *Int J Mol Sci* 20:3328.
- Kerr N, Lee SW, Perez-Barcena J, Crespi C, Ibañez J, Bullock MR, Dietrich WD, Keane RW, de Rivero Vaccari JP (2018) Inflammasome proteins as biomarkers of traumatic brain injury. *PLoS One* 13:e0210128.
- Kovacs SB, Miao EA (2017) Gasdermins: effectors of pyroptosis. *Trends Cell Biol* 27:673-684.
- Kulbe JR, Hall ED (2017) Chronic traumatic encephalopathy-integration of canonical traumatic brain injury secondary injury mechanisms with tau pathology. *Prog Neurobiol* 158:15-44.
- Li XL, Wang B, Yang FB, Chen LG, You J (2022) HOXA11-AS aggravates microglia-induced neuroinflammation after traumatic brain injury. *Neural Regen Res* 17:1096-1105.
- Liu HD, Li W, Chen ZR, Hu YC, Zhang DD, Shen W, Zhou ML, Zhu L, Hang CH (2013) Expression of the NLRP3 inflammasome in cerebral cortex after traumatic brain injury in a rat model. *Neurochem Res* 38:2072-2083.
- Liu L, Arun A, Ellis L, Peritore C, Donmez G (2014) SIRT2 enhances 1-methyl-4-phenyl-1,2,3,6-tetrahydropyridine (MPTP)-induced nigrostriatal damage via apoptotic pathway. *Front Aging Neurosci* 6:184.
- Liu W, Chen Y, Meng J, Wu M, Bi F, Chang C, Li H, Zhang L (2018a) Ablation of caspase-1 protects against TBI-induced pyroptosis in vitro and in vivo. *J Neuroinflammation* 15:48.
- Liu YL, Yuan F, Yang DX, Xu ZM, Jing Y, Yang GY, Geng Z, Xia WL, Tian HL (2018b) Adjuvant attenuates cerebral edema and improves neurological function in mice with experimental traumatic brain injury. *J Neurotrauma* 35:2850-2860.
- Ma MW, Wang J, Dhandapani KM, Brann DW (2017a) NADPH oxidase 2 regulates nlrp3 inflammasome activation in the brain after traumatic brain injury. *Oxid Med Cell Longev* 2017:6057609.
- Ma MW, Wang J, Zhang Q, Wang R, Dhandapani KM, Vadlamudi RK, Brann DW (2017b) NADPH oxidase in brain injury and neurodegenerative disorders. *Mol Neurodegener* 12:7.
- Miao EA, Rajan JV, Aderem A (2011) Caspase-1-induced pyroptotic cell death. *Immunol Rev* 243:206-214.
- Misawa T, Takahama M, Kozaki T, Lee H, Zou J, Saitoh T, Akira S (2013) Microtubule-driven spatial arrangement of mitochondria promotes activation of the NLRP3 inflammasome. *Nat Immunol* 14:454-460.
- Morganti-Kossmann MC, Sempke BD, Hellewell SC, Bye N, Ziebell JM (2019) The complexity of neuroinflammation consequent to traumatic brain injury: from research evidence to potential treatments. *Acta Neuropathol* 137:731-755.
- O'Brien WT, Pham L, Symons GF, Monif M, Shultz SR, McDonald SJ (2020) The NLRP3 inflammasome in traumatic brain injury: potential as a biomarker and therapeutic target. *J Neuroinflammation* 17:104.
- Patel VP, Chu CT (2014) Decreased SIRT2 activity leads to altered microtubule dynamics in oxidatively-stressed neuronal cells: implications for Parkinson's disease. *Exp Neurol* 257:170-181.
- Percie du Sert N, Hurst V, Ahluwalia A, Alam S, Avey MT, Baker M, Browne WJ, Clark A, Cuthill IC, Dirnagl U, Emerson M, Garner P, Holgate ST, Howells DW, Karp NA, Lázic SE, Lidster K, MacCallum CJ, Macleod M, Pearl EJ, et al. (2020) The ARRIVE guidelines 2.0: Updated guidelines for reporting animal research. *PLoS Biol* 18:e3000410.
- Ross J, Brough D, Gibson RM, Loddick SA, Rothwell NJ (2007) A selective, non-peptide caspase-1 inhibitor, VRT-018858, markedly reduces brain damage induced by transient ischemia in the rat. *Neuropharmacology* 53:638-642.
- Saatman KE, Feeko KJ, Pape RL, Raghupathi R (2006) Differential behavioral and histopathological responses to graded cortical impact injury in mice. *J Neurotrauma* 23:1241-1253.
- Schneider CA, Rasband WS, Eliceiri KW (2012) NIH Image to ImageJ: 25 years of image analysis. *Nat Methods* 9:671-675.
- Shaheen MJ, Bekdash AM, Itani HA, Borjac JM (2021) Saffron extract attenuates neuroinflammation in rmTBI mouse model by suppressing NLRP3 inflammasome activation via SIRT1. *PLoS One* 16:e0257211.
- Sun Z, Nyanzu M, Yang S, Zhu X, Wang K, Ru J, Yu E, Zhang H, Wang Z, Shen J, Zhuge Q, Huang L (2020) VX765 attenuates pyroptosis and HMGB1/TLR4/NF- $\kappa$ B pathways to improve functional outcomes in TBI mice. *Oxid Med Cell Longev* 2020:7879629.
- Sutterwala FS, Ogura Y, Szczepanik M, Lara-Tejero M, Lichtenberger GS, Grant EP, Bertin J, Coyle AJ, Galán JE, Askenase PW, Flavell RA (2006) Critical role for NALP3/CIAS1/Cryopyrin in innate and adaptive immunity through its regulation of caspase-1. *Immunity* 24:317-327.
- Swanson KV, Deng M, Ting JP (2019) The NLRP3 inflammasome: molecular activation and regulation to therapeutics. *Nat Rev Immunol* 19:477-489.
- Sweeney MD, Zhao Z, Montagne A, Nelson AR, Zlokovic BV (2019) Blood-brain barrier: from physiology to disease and back. *Physiol Rev* 99:21-78.
- Wang B, Zhang Y, Cao W, Wei X, Chen J, Ying W (2016) SIRT2 plays significant roles in lipopolysaccharides-induced neuroinflammation and brain injury in mice. *Neurochem Res* 41:2490-2500.
- Wang D, Xu X, Wu YG, Lyu L, Zhou ZW, Zhang JN (2018) Dexmedetomidine attenuates traumatic brain injury: action pathway and mechanisms. *Neural Regen Res* 13:819-826.
- Wang Y, Yang J, Hong T, Chen X, Cui L (2019) SIRT2: Controversy and multiple roles in disease and physiology. *Ageing Res Rev* 55:100961.
- Wu D, Lu W, Wei Z, Xu M, Liu X (2018) Neuroprotective effect of Sirt2-specific inhibitor AK-7 against acute cerebral ischemia is P38 activation-dependent in mice. *Neuroscience* 374:61-69.
- Xie XQ, Zhang P, Tian B, Chen XQ (2017) Downregulation of NAD-dependent deacetylase SIRT2 protects mouse brain against ischemic stroke. *Mol Neurobiol* 54:7251-7261.
- Xing Y, Yao X, Li H, Xue G, Guo Q, Yang G, An L, Zhang Y, Meng G (2017) Cutting edge: TRAF6 mediates TLR/IL-1R signaling-induced nontranscriptional priming of the NLRP3 inflammasome. *J Immunol* 199:1561-1566.
- Xiong Y, Mahmood A, Chopp M (2013) Animal models of traumatic brain injury. *Nat Rev Neurosci* 14:128-142.
- Xu X, Yin D, Ren H, Gao W, Li F, Sun D, Wu Y, Zhou S, Lyu L, Yang M, Xiong J, Han L, Jiang R, Zhang J (2018) Selective NLRP3 inflammasome inhibitor reduces neuroinflammation and improves long-term neurological outcomes in a murine model of traumatic brain injury. *Neurobiol Dis* 117:15-27.
- Xu Z, Liu Y, Yang D, Yuan F, Ding J, Chen H, Tian H (2017a) Sesamin protects SH-SY5Y cells against mechanical stretch injury and promoting cell survival. *BMC Neurosci* 18:57.
- Xu ZM, Yuan F, Liu YL, Ding J, Tian HL (2017b) Glibenclamide attenuates blood-brain barrier disruption in adult mice after traumatic brain injury. *J Neurotrauma* 34:925-933.
- Yang DX, Jing Y, Liu YL, Xu ZM, Yuan F, Wang ML, Geng Z, Tian HL (2019a) Inhibition of transient receptor potential vanilloid 1 attenuates blood-brain barrier disruption after traumatic brain injury in mice. *J Neurotrauma* 36:1279-1290.
- Yang Y, Wang H, Kouadir M, Song H, Shi F (2019b) Recent advances in the mechanisms of NLRP3 inflammasome activation and its inhibitors. *Cell Death Dis* 10:128.
- Zhi JJ, Du CZ, Wang YZ (2021) Pyroptosis in the progression of osteoarthritis. *Zhongguo Zuzhi Gongcheng Yanjiu* 25:5204-5209.
- Zhu W, Han B, Fan M, Wang N, Wang H, Zhu H, Cheng T, Zhao S, Song H, Qiao J (2019) Oxidative stress increases the 17,20-lyase-catalyzing activity of adrenal P450c17 through p38 $\alpha$  in the development of hyperandrogenism. *Mol Cell Endocrinol* 484:25-33.

*P-Reviewers: Weng C, Ding F, Donato R; C-Editor: Zhao M; S-Editors: Yu J, Li CH; L-Editors: Yu J, Song LP; T-Editor: Jia Y*